

Accepted Manuscript

This is a post-peer-review, pre-copyedit version of an article published in Environmental Processes by Springer. The final authenticated version is available online at:

<http://dx.doi.org/10.1007/s40710-017-0262-7>

Escudero-Oñate, C., Poch, J. & Villaescusa, I. Environ. Process. (2017) 4: 833.

It is recommended to use the published version for citation.

[Click here to view linked References](#)

Adsorption of Cu(II), Ni(II), Pb(II) and Cd(II) from ternary mixtures: modelling competitive breakthrough curves and assessment of sensitivity

Carlos Escudero-Oñate^{*a}, Jordi Poch^b, Isabel Villaescusa^c

Running head title: Metal sorption from ternary mixtures: modelling and sensitivity.

^a Norwegian Institute for Water Research (NIVA), Gaustadalléen 21, NO-0349 Oslo (Norway)

^b Applied Mathematics Department, Escola Politècnica Superior, Universitat de Girona, c/ M^a Aurèlia Capmany,
61, 17071 Girona (Spain)

^c Chemical Engineering Department, Escola Politècnica Superior, Universitat de Girona, c/ M^a Aurèlia Capmany,
61, 17071 Girona (Spain)

*Corresponding author. Tel.: +47 98215448; fax: +47 22185200

e-mail: carlos.escudero@niva.no

Orcid ID: orcid.org/0000-0002-5871-8862



Abstract

This study describes the competitive sorption of Cu(II), Ni(II), Pb(II) and Cd(II) onto grape stalks wastes (GS) in ternary mixtures in a continuous bed up-flow system. The characteristic breakthrough profile was observed for just one of the metals while the other two suffered overshoots. The elution profile showed that (i) lead is not overshoot in any mixture, (ii) copper overshoots when lead occurs in the ternary mixture and (iii) cadmium and nickel exhibit intense overshoots when either lead or copper are present. A kinetic model based in the Homogeneous Surface Diffusion Model (HSDM) was developed to describe the sorption profile of each metal in the mixtures. To simulate the breakthrough curves, the Extended Langmuir Model (MEL) has been incorporated into the HSDM to describe the equilibrium. The values of the Langmuir affinity constant, b , were found to follow the next ranking: Pb (54.5 ± 0.2) >> Cu (15.2 ± 0.3) >> Cd (9.4 ± 0.1) > Ni (8.1 ± 0.2). These constants successfully explain the competence that leads to the observed overshoots in the mixtures. The model successfully fits metal sorption kinetics and elution profile in the mixtures. A study of the model sensitivity was carried out to know how the uncertainty in the experimental data and the model parameters affect the uncertainty in the output of the model. This analysis highlighted the relevance of good estimation of K_{max} , b and η besides the need of gathering high quality experimental data for an accurate determination of the model parameters.

Keywords: Homogeneous Surface Diffusion Model, metals, overshoot, grape stalks, packed column, sensitivity analysis

1. Introduction

Toxic metal pollution is a worldwide environmental problem; their immutable nature, high mobility and toxicity to live organisms have made them a priority in environmental management. When water is polluted with potentially toxic metals, it can be detrimental and even lethal to living organisms. Moreover, their discharge over land enables them to be sorbed by various components in soil and then re-adsorbed via crops into the animal and human food chains (Swati and Hait 2017)

There are many industrial sources of metal pollution, including manufacturing processes such as smelting and refining, electricity generation and nuclear power, tanneries, battery manufacturing and textile activities, but also natural pollution sources such as it is the case of the acid mine drainage are relevant (Akcil and Koldas 2006; Nguyen et al. 2015). The increasing harshness in the regulations related to environmental discharges of potentially toxic metals to the environment makes this kind of pollutants priority substances to be kept under control. Among the most frequently found in industrial operations or in mining drainage are Cu(II), Ni(II), Pb(II) and Cd(II). All of them are recognized as hazardous pollutants and their environmental release and dispersion has to be strictly controlled.

Lead is the oldest known toxic metal and exposure to this metal can mainly occur through drinking water, smoking or even due to various industrial processes like smelting, through battery recycling. As it does not have any biological function, even at low levels, it can affect multiple clinical functions. Its most prominent effect is on the oxidative stress mechanism, wherein antioxidants like glutathione within the cell protect from cellular damage induced by the reactive oxygen species (Iyer et al. 2015). Cu is well known as a promoter of oxidative damage in conditions of increased levels in the liver and brain. The best known disorder associated to Cu dyshomeostasis is Wilson's disease, an autosomal recessive disorder linked to the Cu translocase expressed in hepatocytes (Boveris et al. 2012). Cu toxicity has been linked to cancer progression, cardiovascular disease, atherosclerosis, diabetes and especially to neurological disorders (Jomova and Valko 2011). Nickel above critical level can provoke serious lung and kidney problems aside from gastrointestinal distress, pulmonary fibrosis, skin dermatitis (Borba et al. 2006) and is suspected to be a potential human carcinogen (Chiou et al. 2015). Cadmium has been classified by U.S. Environmental Protection Agency as a probable human carcinogen and exposure to it can seriously threat human health. Chronic exposure to cadmium results in kidney dysfunction and high levels of exposure will result in death (Fu and Wang 2011).

Different methods to remove potentially toxic metals from aqueous solutions exist nowadays. Among them, the most widely used are based in precipitation, coagulation/flocculation, ion exchange, reverse osmosis, nano-

filtration, solvent extraction and adsorption (Femina Carolin et al. 2017). The main drawbacks of the
 aforementioned technologies derive from the high implementation and operation costs, especially when the
 concentration of the target metal is below 100 mg L⁻¹. To overcome the problem of the exploitation costs when it
 comes to detoxification of effluents polluted with toxic metals, many researchers have explored the use of
 natural, readily available materials as biosorbents. Biosorbents are prepared from either waste/abundant
 materials or using low-cost cultivation techniques, thus decreasing the process cost and making the process eco-
 friendly (Vijayaraghavan and Balasubramanian 2015). Among the different potential sources of these materials,
 agro-industrial activities act as a vast, reliable and constant source of natural resources potentially useful for the
 removal of metals from polluted streams (Chao et al. 2014; Esfandiar et al. 2014; Ghasemi et al. 2014; Moyo et
 al. 2015; Simate and Ndlovu 2015). That is the case of a special sub-group in the agro-industrial by-products; the
 lignocellulosic wastes. These kind of materials, mostly formed by cellulose, hemicellulose and lignin (Abdolali
 et al. 2014) have demonstrated good sorption capacity for different metals. This is the case of the removal of Pb
 by olive stones (Blázquez et al. 2014), Cd, Pb and Zn by agave bagasse (Velazquez-Jimenez et al. 2013), Cr(VI)
 by exhausted coffee wastes (Fiol et al. 2008) and grape stalks (Escudero et al. 2009; Fiol et al. 2006), Cu by
 yohimbe bark (Escudero et al. 2008), pine cone shell (Martín-Lara et al. 2016) and sawdust (Djeribi and
 Hamdaoui 2008; Larous and Menia 2012).
 Despite sorption onto natural biomaterials has demonstrated to be an effective method to detoxify metal polluted
 streams, just few authors have tackled one of the most realistic scenarios relevant to industrial implementation of
 this technology: multimetal solution and operation in continuous bed up-flow process (in analogy to the current
 use and exploitation of commercial ion exchangers). The multi-element scenario is of major concern, since real
 polluted streams involve multimetal “cocktails” where competitive sorption interactions may take place. For
 example, the sorption of Cu(II) and Pb(II) from their binary mixtures using pine cone shell in a continuous bed
 up-flow process has been explored (Martín-Lara et al. 2016), being reported a higher selectivity for Pb(II) over
 Cu(II) ions. The sorption behaviour of bone char in a continuous bed up-flow system in binary mixtures Cd/Cu
 and Cu/Zn has also been reported (Ko et al. 2005). Also, the competitive adsorption of Cu(II) and Ni(II) onto a
 marine algae, *Sargassum filipendula* has been previously explored (Kleinübing et al. 2011). The authors reported
 a preferential sorption of Cu(II) over Ni(II) that concluded in the displacement of Ni(II) and the subsequent
 formation of a marked overshoot in the outlet stream.
 Previous studies put into evidence that sorption of Cu(II), Ni(II), Pb(II) and Cd(II) onto grape stalks wastes in
 binary mixtures in a continuous bed up-flow system is a competitive process. This competition is observed

through an overshoot in the breakthrough curve, i.e., a sudden increase above the input concentration to decrease later to its inlet stream concentration level. The overshoot effect is strongly dependent on the selectivity of the sorbent through the different sorbates, the sorption mechanism and on the operational conditions imposed. If the operational condition is the one that minimizes the mass transfer resistances of one of the sorbates, it is expected a pronounced overshooting when the optimal operational conditions of the other sorbates are different from the one of interest (Barros, 2013). In equimolar multimetal solutions, the overshoot metals are those whose interaction with the sorbent are weaker in a process that involves the replacement from their coordinating positions by a metal through which the sorbent shows a higher affinity.

In this paper, we investigate the use of a GS-based sorbent for the removal of Cu(II), Ni(II), Pb(II) and Cd(II) in all their possible ternary mixtures and in a fixed bed up-flow system. A model based on the Homogeneous Surface Diffusion Model has been developed to describe competitive sorption of the four metal ions in all their possible ternary mixtures. A study of the model sensitivity was carried out to know how the uncertainty in the experimental data and the model parameters affect the uncertainty in the output of the model.

2. Experimental

2.1 Materials, Reagents and Instrumentation

Grape stalks (GS) wastes (by product generated in industrial wine production) were supplied by a wine manufacturer from Castilla la Mancha region (Spain). The material was rinsed three times with distilled water, dried in an oven at 110 °C until constant weight, cut and sieved for a particle size of 0.25-0.50 mm. Stock solutions of Cu(II), Ni(II), Pb(II) and Cd(II) (1000 mg L⁻¹) were prepared by dissolving appropriate amounts of CuCl₂·2H₂O, NiCl₂·6H₂O, PbCl₂, CdCl₂·2·1/2H₂O in high purity water (Milli-Q, Millipore Corp.). The stock solutions were further mixed and diluted to obtain 0.2 mM concentration on each metal.

Metal concentration in solution was analysed by Flame Atomic Absorption Spectroscopy (FAAS) using a Varian SpectrAA 220FS coupled to an automatic dilutor Varian SIPS and an autosampler Varian SPS3. The metals were nebulized in a concentric pneumatic system and atomized in an air-acetylene flame. Lead, cadmium, copper and nickel hollow cathode lamps were used as light sources for the selective detection of the metals and standard solutions of 1000 mg L⁻¹ were used for FAAS calibration. Measurement of pH was performed using a pHmeter PHM 250 (Meterlab).

2.2 Metal Sorption from Ternary Mixtures

Mixtures Cu(II)-Ni(II)-Cd(II), Cu(II)-Pb(II)-Cd(II), Cu(II)-Pb(II)-Ni(II) and Pb(II)-Ni(II)-Cd(II) were prepared mixing appropriate volumes of single stock solutions and diluting with Milli-Q water. The pH of the different ternary mixtures prepared was adjusted to 5.2 by adding negligible amounts of concentrated NaOH. GS wastes were soaked in Milli-Q water in a ratio 20:1 (water V (mL):GS mass (g)) under continuous magnetic stirring for 48 hours to allow both: free swell up of the material prior to column filling and removal of the finest particles that might cause clogging of the GS bed, tubes and valves. The experiments were performed in a borosilicate column (Omifit, 10 cm length x 1 cm inner diameter) filled with 0.5 g of GS. Glass beads were placed in the bottom of the column to act as diffuser and help in the homogenization of the stream right before getting in contact with the GS bed. The column was operated in up-flow mode. A peristaltic pump (Gilson Minipuls) was attached to the bottom of the column and was programmed to deliver a constant flow rate of 30.0 mL h⁻¹. The different ternary mixture solutions were pumped upwards and sampling was carried out automatically using an autosampler (Gilson FC203B) programmed to collect 5.5 mL of the outlet stream in time intervals of 30 minutes. The samples eluted from the column were immediately acidified adding 5 µL of concentrated nitric acid (HNO₃ suprapur, Panreac) and stored until analysis by Flame Atomic Absorption Spectrometry. Characteristic breakthrough curves for each one of the metals forming the ternary mixtures were obtained by plotting the eluted concentration as a function of time. Each experiment was carried out in duplicate and the average results are presented.

2.3. Calculation of the Bed Porosity

The characteristic bed porosity (ϵ) was calculated right before the sorption experiments. Water was pumped throughout all the tubes to ensure that all the channels were primed. When the liquid reached the bottom of the sorbent bed, time was set to 0 and the required time to fill up the column was recorded. The void volume V_v (mL) was calculated according to the expression:

$$V_v = Q_v t \quad (1)$$

being Q_v the volumetric flow (mL min⁻¹), and t (min) the time required to fill up the column bed with water. The porosity was calculated through the equation:

$$\epsilon = \frac{V_v}{V_c} \quad (2)$$

where V_c (mL) is the volume of the sorbent bed in the column.

2.4. Calculation of the Sorbed Amount in the Bed

The accumulated amount of copper, nickel, lead and cadmium in the column ($\bar{q}(t)$, mmol g⁻¹) was calculated from the data of the concentration in the outlet stream as a function of time.

$$\bar{q}(t) = \frac{C_F Q_v}{1000 m} \int_0^t \left(1 - \frac{C(t)|_{z=l}}{C_F} \right) dt \quad (3)$$

In the aforementioned equation, m is the dry mass of GS (g), C_F is the feeding concentration (mmol L⁻¹), Q_v is the volumetric flow rate (mL min⁻¹), and $C(t)|_{z=l}$ is the outlet metal concentration (mmol L⁻¹). The integral part of the equation was numerically solved using the trapeze method.

2.5. Quality Assurance

To assure the accuracy, reliability and reproducibility of the raw data, the sorption assays were run in duplicate and average values are reported. All the chemicals (AR grade) were purchased from reliable suppliers with certified quality. All the glassware and plastic material was previously soaked in 0.1 M HNO₃, rinsed thoroughly with Milli-Q water and dried in an oven at 85 °C. Calibration was performed in the range 0.1-50 mg·L⁻¹ using a Cu(II), Ni(II), Pb(II) and Cd(II) mixture prepared from individual solutions of certified standards. The accuracy was checked assessing the relative standard deviation (RSD) of each sample analysis. Typical values of the RSD for the target metals were below 5% in the samples and lower than 2.5 % in the standard solutions.

2.6 Modelling of Sorption Process

2.6.1 Equilibrium Models

The sorption equilibrium isotherm of each metal in the ternary mixtures was described according to the Modified Extended Langmuir (MEL) (Choy et al. 2000; Ghaedi et al. 2014; Kurniawan et al. 2012; Muhammad et al. 2011; Park et al. 2012; Valderrama et al. 2010; Xia et al. 2014), based on the mechanism of direct competition for adsorption sites, and whose mathematical expression is:

$$q_{e,i} = \frac{K_{max,i} b_i \left(\frac{C_{e,i}}{\eta_i} \right)}{1 + \sum_{j=1}^n b_j \left(\frac{C_{e,j}}{\eta_j} \right)} \quad (4)$$

The development of Eq. (4) for the three metals competing in the ternary mixture, gives a set of equations:

$$q_{e,1} = \frac{K_{max,1}b_1(C_{e,1}/\eta_1)}{1 + b_1(C_{e,1}/\eta_1) + b_2(C_{e,2}/\eta_2) + b_3(C_{e,3}/\eta_3)} \quad (5)$$

$$q_{e,2} = \frac{K_{max,2}b_2(C_{e,2}/\eta_2)}{1 + b_1(C_{e,1}/\eta_1) + b_2(C_{e,2}/\eta_2) + b_3(C_{e,3}/\eta_3)} \quad (6)$$

$$q_{e,3} = \frac{K_{max,3}b_3(C_{e,3}/\eta_3)}{1 + b_1(C_{e,1}/\eta_1) + b_2(C_{e,2}/\eta_2) + b_3(C_{e,3}/\eta_3)} \quad (7)$$

where $q_{e,i}$ are the equilibrium solid-phase concentration (mmol g^{-1}), $K_{max,i}$ are the MEL constants (L mg^{-1}), η_i are the Langmuir correction coefficients, and b_i the Langmuir isotherm constants (L mmol^{-1}). The Langmuir correction coefficient (η) represents the competitive effect between components of the mixture.

2.6.2 Fixed-bed Model

In the process of adsorption in continuous bed up-flow systems, the following physicochemical processes should be considered:

- i) The mechanisms of mass transport in the liquid phase are convection/advection, axial and radial dispersion.
- ii) Film diffusion from the liquid to the solid phase.
- iii) Pore diffusion (diffusion in the liquid to fill the wells of the particle).
- iv) Adsorption/desorption on the sorbent sites.
- v) Surface diffusion (spreading of the transferred solutes on the surface of the pores).

Incorporating all these phenomena in a model is complex due to the large number of parameters that should be determined (radial and axial dispersion coefficients, mass transfer, pore diffusion, surface adsorption and desorption of each sorbate, etc.). Moreover, these parameters cannot be determined with experiments on an adsorption column and the effects of these processes on the breakthrough curves are very similar.

Therefore, to describe the processes occurring inside the particles, simplified models such as the Homogeneous Surface Diffusion Model (HSDM) (Lee and McKay 2004; Valderrama et al. 2010) or Pore Diffusion Model (PDM) (Ko et al. 2001; Traylor et al. 2014; Liu 2010) have been proposed. In these models, pore and surface diffusion are assimilated into a single effective diffusion. To describe the mass transport in the column, it is common to postulate that all cross-sections are homogeneous and the radial movement and axial dispersion could be neglected.

In this work, the sorption of Cu(II), Ni(II), Pb(II) and Cd(II) in the ternary mixtures was assessed and modelled according to the Homogeneous Surface Diffusion Model (HSDM) (Ko et al. 2004). The hypothesis in which the HSDM model relies are the following (Richard et al. 2010):

(1) Fluid moves in one-dimensional regime under plug-flow conditions

(2) The particles behave as a pseudo-homogeneous medium wherein the pollutant diffuses.

(3) External mass-transfer limitation is accounted for.

(4) Adsorption equilibrium prevails at the fluid-solid external surface

In accordance with these assumptions and mass transport mechanisms, the following set of mathematical equations can be derived. The mass balance for each component i of the bulk liquid phase in the column is expressed by the following equation:

$$\frac{\partial C_i}{\partial t} = -v \frac{\partial C_i}{\partial z} - \rho \left(\frac{1 - \varepsilon}{\varepsilon} \right) \frac{\partial q_i}{\partial t} \quad (8)$$

where v is the linear flow rate in the column, z is the bed depth, t is the service time, ρ is the particle density of grape stalks, ε is the porosity of the bed, C_i is the liquid-phase concentration and q_i is the solid-phase concentration.

Since the rate of accumulation of solute in the solid surface is equal to the rate of transfer of solute across the liquid film, the mass balance through the stagnant liquid film for each component i is:

$$\rho \frac{\partial q_i}{\partial t} = \frac{3k_{f,i}}{R} (C_i - C_{s,i}) \quad (9)$$

where $k_{f,i}$ is the external film transport coefficient, R is the particle radius and $C_{s,i}$ is the liquid-phase concentration at the particle surface.

Substituting (9) into (8) results in:

$$\frac{\partial C_i}{\partial t} = -v \frac{\partial C_i}{\partial z} - \left(\frac{1 - \varepsilon}{\varepsilon} \right) \frac{3k_{f,i}}{R} (C_i - C_{s,i}) \quad (10)$$

For spherical sorbent particles using surface diffusion as the major intraparticle transport mechanism, the ternary Fickian diffusion equations are:

$$\frac{\partial q_i}{\partial t} = \frac{1}{r^2} \frac{\partial}{\partial r} \left(r^2 \sum_{j=1}^3 D_{s,ij} \frac{\partial q_j}{\partial r} \right) \quad (11)$$

where r is the position inside the particle, $D_{s,ij}$ are the multicomponent diffusion coefficients in the solid phase.

In ternary mixtures, the cross-term diffusivities, $D_{s,12}$, $D_{s,13}$, $D_{s,21}$, $D_{s,23}$, $D_{s,31}$ and $D_{s,32}$ give the measure of the flux of one solute that is provoked by the concentration gradient of a second solute. Assuming that the effect of these cross-term diffusivities is small, and therefore their contributions to the overall diffusion is negligible, the above equations can be simplified to Eq. (12):

$$\frac{\partial q_i}{\partial t} = \frac{1}{r^2} \frac{\partial}{\partial r} \left(r^2 D_{s,ii} \frac{\partial q_i}{\partial r} \right) \quad (12)$$

with the boundary conditions at the center and surface of the particle,

$$\left. \frac{\partial q_i}{\partial r} \right|_{r=0} = 0, \quad t \geq 0 \quad (13)$$

$$D_{s,ii} \left. \frac{\partial q_i}{\partial r} \right|_{r=R} = \frac{k_{f,i}}{\rho} (C_i - C_{s,i}), \quad t \geq 0 \quad (14)$$

and the initial condition

$$q_i = 0, \quad t = 0 \text{ and } 0 \leq r \leq R \quad (15)$$

$$C_i = 0, \quad t = 0 \text{ and } z > 0 \quad (16)$$

with the boundary condition at the input column flow,

$$C_i = C_{F,i}, \quad t \geq 0, z = 0 \quad (17)$$

The coupling equation between the solid and liquid concentration is the equilibrium isotherm. Therefore, $C_{s,i}$ can be calculated assuming equilibrium at the particle surface. In ternary metal sorption systems:

$$C_{s,i} = f_i^{-1}(q_{e,1}, q_{e,2}, q_{e,3}) \quad (18)$$

where f_i^{-1} is the inverse of Eqs. (5), (6) and (7), respectively, q_{e1} and q_{e2} and q_{e3} are $q_1(R)$, $q_2(R)$ and $q_3(R)$ calculated in Eq. (8).

The simulation model -based on the incorporation of the Modified Extended Langmuir (MEL) into the kinetic HSDM- was written in Matlab R2013 and used for breakthrough curves prediction in the ternary systems. The numerical solutions of the system of partial differential equations (Eqs. 10, 12) with the boundary and initial conditions (Eqs. 14-17) were solved by using a finite difference method. Equation (10), which represents the mass balance of each component, has been solved by applying a forward difference scheme. Equation (12), that represents the surface diffusion in the solid phase, has been solved by using the Crank–Nicolson method (Ko et al. 2003). The parameters of the model were determined by minimizing the Sum of Square Residuals (SSR) (Eq. 19).

$$SSR = \sum_{i=1}^n \sum_{j=1}^N \left(C_i(t_j, L) - C_{i,exp}(t_j) \right)^2 \quad (19)$$

$$MSSR = SSR/nN \quad (20)$$

where n is the number of metal ions, and N the number of experimental data; C_i is the concentration at time t_j in the outlet flow calculated by the model, and $C_{i,exp}$ is the experimental concentration at time t_j . Minimization of the SSR was carried out by using genetic algorithm (GA) (*ga* function) and the *fmincon* function of the Optimization Toolbox from Matlab 2013 package. The first function was used to obtain a first estimation of the parameters values and the later to refine the results. The *fmincon* of Matlab is a function to find minimum of

constrained nonlinear multivariable function and the different optimization algorithms. In the work presented in this manuscript we used the algorithm “interior-point”.

3. Results and Discussion

3.1 Metal Sorption from Ternary Mixtures

Breakthrough curves were obtained by plotting the outlet stream concentration (C_i) versus time (t). Experimental sorption data (symbols) of the different ternary mixtures of Pb(II), Cu(II), Cd(II) and Ni(II) are presented in Figure 1. The breakthrough profile shows that in all the ternary systems, just one of the metals exhibits the regular sigmoidal shape. The concentration of the other two metals in the outlet stream always exceeds the feeding concentration, leading to the formation of overshoots in their breakthrough curves. The overshoot phenomenon appears when the sorbent reaches its maximum sorption capacity. From this moment the metal ions with weaker interactions are displaced from the sorbent binding sites and pushed off the column. The results presented in Figure 1 reveal that lead is not overshoot in presence of the other two metals in the ternary mixture and copper is only overshoot when lead is present in the mixture. Cadmium and nickel overshoot to a greater or lesser extent depending on the other metals. These results are in agreement with the rank of affinity sorbent-sorbate (grape stalks-metal) reported in our previous work (Escudero et al. 2013) and by other authors using natural adsorbents (Bayo 2012; Kleinübing et al. 2011). The sorbent-metal affinity can be justified by the degree of complexation exhibited by metals with the binding groups of the sorbent bearing a $-\text{COOH}$ group. According to this type of interaction, the degree of complexation reported by Nurchi et al. (2010) follows the ranking: $\text{Al}, \text{Pb} > \text{Cu} > \text{Cd} > \text{Co}, \text{Mn}, \text{Ni}, \text{Zn}$.

The experimental conditions used in the model for breakthrough prediction are depicted in Table 1. The parameters derived from the optimization of the HSDM (external mass transfer coefficient ($k_{f,i}$), diffusion coefficient ($D_{e,ii}$), MEL constant ($K_{max,i}$), the Langmuir affinity constant (b_i) and the Langmuir correction coefficient (η_i)) are presented in Table 2a. The sum of squares residuals (SSR) and mean sum of square residuals ($MSSR$) obtained from the optimization of the model can be found in Table 2b. The data obtained in single metal solutions under the same experimental conditions have been included for comparison sake in Table 2c. Diffusion and mass transfer coefficient values have the same order of magnitude with those found in our previous study regarding single (Table 2c) and binary mixtures (Escudero et al. 2013), and are also in agreement with those reported by other authors when studying copper biosorption by an algae composite biosorbent in a similar sorption system (Vilar et al. 2008). The values of the Langmuir affinity constant, b , from higher to lower,

were found to be: Pb (54.5 ± 0.2) >> Cu (15.2 ± 0.3) >> Cd (9.4 ± 0.1) > Ni (8.1 ± 0.2). These values successfully explain the overshoots observed in the ternary mixtures. Remarkable are the low values of *SSR* and *MSSR*, indicating the excellent fitting of the model to the experimental results.

The data provided by the model by using the constant values presented in Table 2a are superimposed to the experimental data (line) in Figure 1. As seen in the figure, the model describes very well both: (i) the sorption process followed by each component on the ternary mixture; and (ii) the mass transfer wave observed when plotting the amount of metal ions sorbed as a function of the radius of the particle and the axial position of the column (bed height) (Video provided as supplementary material).

The time-course profile of the metal sorbed amount in the different ternary mixtures is depicted in Figure 2. As seen, the three metal ions are progressively sorbed showing a similar slope until the sorbent capacity is close to achieve its maximum. From this moment, two of the metals (according to their affinity constant) are pushed off leading to the observed overshoot in the outlet effluent and their concentration in the solid phase progressively decreases.

The goodness of the model to describe the sorbed amount at equilibrium for each one of the metals in the ternary mixtures ($q_{e,i}$) was assessed plotting the actual sorbed amount against the predicted by the model (Figure 3). As observed in the figure, all the data are distributed on the bisecting first quadrant (slope 1.007 and $R^2=0.996$), showing that the model provides an excellent prediction of the sorption equilibrium for all the metals, irrespective of whether the metal suffers overshoot or not.

3.2 Model Sensitivity Analysis

The sensitivity of the model to the different parameters was assessed. The parameters (summarized below) are either a characteristic of the mass transfer process or related to the sorption equilibrium.

- D_{s0} ($\text{cm}^2 \text{s}^{-1}$), the effective diffusivity
- k_f (cm s^{-1}), external film transport coefficient
- K_{\max} (mmol g^{-1}): MEL constant
- b (L mmol^{-1}): Langmuir isotherm constant
- η : Langmuir correction coefficient

After fitting a model, it is possible to make predictions. Therefore, it is paramount to assess the performance of these predictions by evaluating the risk of inaccurate outputs. The sensitivity of the model was assessed by two different approaches: The effect on the model output when varying the model parameters and when

experimental data are perturbed. The process of studying the sensitivity of the model with respect to the variation of its parameters ($k_{f,i}$, $D_{s,ii}$, $K_{max,i}$, b_i and η_i) consisted in introducing a $\pm 5\%$ variation in one of the input parameters while keeping the rest constant, and observing the resulting influence on model predictions. This influence was estimated by calculating the variation of the error (SSR_j and VR_j (Eq. 21)) as a measure of the difference between experimental and calculated values (Table 3).

$$VR_j = \frac{SSR_j - SSR}{SSR} 100 \quad (21)$$

where SSR values are the ones presented in Table 2b and SSR_j is the average calculated value resulting from the introduction of the $\pm 5\%$ variation above mentioned. Results presented in Table 3 put into evidence that the model is very sensitive to the variation of $K_{max,i}$ as evidenced by the VR_j values higher than 5%. As seen, these values vary between 8.7 and 126.8%. The other two parameters to which the model is sensitive are b_i and η_i . The VR_j corresponding to these two parameters are higher than 5% except in the case of the ternary mixture Cu-Ni-Cd. Conversely, the model exhibits low sensitivity towards $D_{s,ii}$ and $k_{f,i}$ with values of VR_j lower than 3.3%. These results highlight the importance of getting good estimates of $K_{max,i}$, b_i and η_i .

The sensitivity of the model towards experimental errors was studied by introducing a certain variation ($\pm 2.5\%$), following a normal distribution, in each of the experimental data points. A total of 10 simulations were considered and the corresponding parameters of the model were calculated by following the procedure indicated in section 2.3.2. The mean (\bar{x}) and the standard deviation (s) of each of the parameters values are presented in Table 4.

The results presented in Table 4 show that the effect of the experimental data perturbation is very low on the estimation of the parameters of Pb-Ni-Cd and Cu-Ni-Cd ternary mixtures. In the former mixture the standard deviation values present variations lower than 2.5% of the mean value. In the latest, variations are lower than 5%, except in the case of $D_{s,ii}$ (4.6-12.0%). Variation of b_i is always lower than 2.5% and $K_{max,i}$ and η_i lower than 7.2% in all ternary mixtures. The higher variations are found for $k_{f,i}$ and $D_{s,ii}$ whose percentage of variation goes from 12 to 61% and from 15 to 48% in the ternary mixtures Cu-Pb-Ni and Cu-Pb-Cd, respectively. These results put into evidence that little perturbations of the experimental data result in high variations of $k_{f,i}$ and $D_{s,ii}$. Therefore, ensuring good quality experimental data is essential to get an accurate determination of model parameters.

Conclusions

Sorption of Cu(II), Ni(II), Pb(II) and Cd(II) from ternary mixtures onto grape stalks under continuous bed up-flow conditions is a competitive process. In all the mixtures, the sorption of the metal with higher affinity for the sorbent followed the expected sigmoidal trend while the other two metals showed overshoots. Lead did not experience overshoots in any of the studied ternary systems; copper was only overshoot when lead was present while cadmium and nickel suffered intense overshoots when either, lead or copper were present in the mixture. A kinetic model based on a Homogeneous Surface Diffusion Model was successfully developed to describe the dynamics of metal sorption onto grape stalks in all the ternary mixtures. Despite the complexity that involves the sorption of three metal ions with the formation of two simultaneous overshoots, the model was capable to fit the overall process. The sensitivity analysis of the model highlighted the high relevance of getting good estimates of $K_{max,i}$, b_i and η_i , and the need of gathering high quality experimental data for an accurate determination of the model parameters.

Acknowledgements

This work has been supported by Ministerio de Economía y Competitividad, Spain, ref. CTM2015-68859-C2-1-R. We express also our sincere gratitude to the reviewers for the constructive comments provided in the review of the paper.

Compliance with ethical standards

1. Disclosure of potential conflicts of interest

On behalf of the authors, the corresponding authors declares that there is no conflict of interest

2. Research involving Human Participants and/or Animals

This article does not contain any studies with human participants or animals performed by any of the authors.

3. Informed consent

All authors declare that they have participated sufficiently in the work to take public responsibility for the content, including participation in the concept, design, analysis, writing, and revision of the manuscript. All authors had full access to all of the data in the study and can take responsibility for the integrity of the data and the accuracy of the data analysis. All authors approved the final version. Furthermore, each author certifies that this material has not been and will not be submitted to or published in any other publication.

References

- Abdolali A, Guo WS, Ngo HH, Chen SS, Nguyen NC, Tung KL (2014) Typical lignocellulosic wastes and by-products for biosorption process in water and wastewater treatment: A critical review. *Bioresource Technol* 160:57-66
- Akcil A, Koldas S (2006) Acid Mine Drainage (AMD): causes, treatment and case studies. *J Clean Prod* 14:1139-1145
- Barros MASD, Arroyo PA, Silva EA (ed) (2013) General Aspects of Aqueous Sorption Process in Fixed Beds. InTech, Mass Transfer-Advances in Sustainable Energy and Environment Oriented Numerical Modeling. Chapter 14.
- Bayo J (2012) Kinetic studies for Cd(II) biosorption from treated urban effluents by native grapefruit biomass (*Citrus paradisi* L.): The competitive effect of Pb(II), Cu(II) and Ni(II). *Chem Eng J* 191:278-287
- Blázquez G, Calero M, Ronda A, Tenorio G, Martín-Lara MA (2014) Study of kinetics in the biosorption of lead onto native and chemically treated olive stone. *J Ind Eng Chem* 20:2754-2760
- Borba CE, Guirardello R, Silva EA, Veit MT, Tavares, CRG (2006) Removal of nickel(II) ions from aqueous solution by biosorption in a fixed bed column: Experimental and theoretical breakthrough curves. *Biochem Eng J* 30:184-191
- Boveris A, Musacco-Sebio R, Ferrarotti N, Saporito-Magriñá C, Torti H, Massot F, Repetto MG (2012) The acute toxicity of iron and copper: Biomolecule oxidation and oxidative damage in rat liver. *J Inorg Biochem* 116:63-69
- Chao H-P, Chang CC, Nieva A (2014) Biosorption of heavy metals on *Citrus maxima* peel, passion fruit shell, and sugarcane bagasse in a fixed-bed column. *J Ind Eng Chem* 20:3408-3414
- Chiou YH, Liou SH, Wong RH, Chen CY, Lee H (2015) Nickel may contribute to EGFR mutation and synergistically promotes tumor invasion in EGFR-mutated lung cancer via nickel-induced microRNA-21 expression. *Toxicol Lett* 237:46-54
- Choy KKH, Porter JF, McKay G (2000) Langmuir isotherm models applied to the multicomponent sorption of acid dyes from effluent onto activated carbon. *J Chem Eng Data* 45:575-584
- Djeribi R, Hamdaoui O (2008) Sorption of copper(II) from aqueous solutions by cedar sawdust and crushed brick. *Desalination* 225:95-112
- Escudero C, Fiol N, Poch J, Villaescusa I (2008) The kinetics of copper sorption onto yohimbe bark wastes. *Int J Environ Pollut* 34:215-230
- Escudero C, Fiol N, Poch J, Villaescusa I (2009) Modeling of kinetics of Cr(VI) sorption onto grape stalk waste in a stirred batch reactor. *J Hazard Mater* 170:286-291
- Escudero C, Poch J, Villaescusa I (2013) Modelling of breakthrough curves of single and binary mixtures of Cu(II), Cd(II), Ni(II) and Pb(II) sorption onto grape stalks waste. *Chem Eng J* 217:129-138
- Esfandiar N, Nasernejad B, Ebadi T (2014) Removal of Mn(II) from groundwater by sugarcane bagasse and activated carbon (a comparative study): Application of response surface methodology (RSM). *J Ind Eng Chem* 20:3726-3736
- Femina Carolin C, Senthil Kumar P, Saravanan A, Janet Joshiba G, Naushad Mu (2017) Efficient techniques for the removal of toxic heavy metals from aquatic environment: A review. *J Environ Chem Eng* 5: 2782-2799.
- Fiol N, Escudero C, Poch J, Villaescusa, I (2006) Preliminary studies on Cr(VI) removal from aqueous solution using grape stalk wastes encapsulated in calcium alginate beads in a packed bed up-flow column. *React Funct Polym* 66:795-807
- Fiol N, Escudero C, Villaescusa I (2008) Re-use of exhausted ground coffee waste for Cr(VI) sorption. *Sep Sci Technol* 43:582-596
- Fu F, Wang Q (2011) Removal of heavy metal ions from wastewaters: a review. *J Environ Manage* 92:407-418
- Ghaedi M, Pakniat M, Mahmoudi Z, Hajati S, Sahraei R, Daneshfar A (2014) Synthesis of nickel sulfide nanoparticles loaded on activated carbon as a novel adsorbent for the competitive removal of Methylene blue and Safranin-O. *Spectrochim Acta A-M* 123:402-409
- Ghasemi M, Naushad M, Ghasemi N, Khosravi-fard Y (2014) A novel agricultural waste based adsorbent for the removal of Pb(II) from aqueous solution: Kinetics, equilibrium and thermodynamic studies. *J Ind Eng Chem* 20:454-461
- Iyer S, Sengupta C, Velumani A (2015) Lead toxicity: An overview of prevalence in Indians. *Clin Chim Acta* 451, Part B:161-164
- Jomova K, Valko M (2011) Advances in metal-induced oxidative stress and human disease. *Toxicology* 283:65-87
- Kleinübing SJ, Da Silva EA, Da Silva MGC, Guibal E (2011) Equilibrium of Cu(II) and Ni(II) biosorption by marine alga *Sargassum filipendula* in a dynamic system: Competitiveness and selectivity. *Bioresource Technol* 102:4610-4617
- Ko DCK, Cheung CW, Choy KKH, Porter JF, McKay G (2004) Sorption equilibria of metal ions on bone char. *Chemosphere* 54:273-281

- Ko DCK, Porter JF, McKay G (2005) Application of the concentration-dependent surface diffusion model on the multicomponent fixed-bed adsorption systems. *Chem Eng Sci* 60:5472-5479
- Ko DCK, Porter JF, McKay G (2001) Film-pore diffusion model for the fixed-bed sorption of copper and cadmium ions onto bone char. *Water Res* 35:3876-3886
- Ko DCK, Porter JF, McKay G (2003) Mass transport model for the fixed bed sorption of metal ions on bone char. *Ind Eng Chem Res* 42:3458-3469
- Kurniawan A, Sutiono H, Indraswati N, Ismadji S (2012) Removal of basic dyes in binary system by adsorption using rarasaponin–bentonite: revisited of extended Langmuir model. *Chem Eng J* 189–190:264-274
- Larous S, Menia IH (2012) Removal of copper (II) from aqueous solution by agricultural by-products-sawdust. *Energy Proced* 18:915-923
- Lee VKC, McKay G (2004) Comparison of solutions for the homogeneous surface diffusion model applied to adsorption systems. *Chem Eng J* 98:255-264
- Liu B, Zeng L, Mao J, Ren Q (2010) Simulation of levulinic acid adsorption in packed beds using parallel pore/surface diffusion model. *Chem Eng Technol* 33:1146-1152
- Martín-Lara MA, Blázquez G, Calero M, Almendros AI, Ronda A (2016) Binary biosorption of copper and lead onto pine cone shell in batch reactors and in fixed bed columns. *Int J Min Process* 148:72-82
- Moyo M, Guyo U, Mawenyiyo G, Mawenyiyo G, Ngceboyakwethu PZ, Nyamunda BC (2015) Marula seed husk (*Sclerocarya birrea*) biomass as a low cost biosorbent for removal of Pb(II) and Cu(II) from aqueous solution. *J Ind Eng Chem* 27:126-132
- Muhammad, Chuah TG, Robiah Y, Suraya, AR, Choong TSY (2011) Single and binary adsorption isotherms of Cd(II) and Zn(II) on palm kernel shell based activated carbon. *Desalin Water Treat* 29:140-148
- Nguyen VK, Lee MH, Park HJ, Lee JU (2015) Bioleaching of arsenic and heavy metals from mine tailings by pure and mixed cultures of *Acidithiobacillus* spp. *J Ind Eng Chem* 21:451-458
- Nurchi VM, Crisponi G, Villaescusa I (2010) Chemical equilibria in wastewaters during toxic metal ion removal by agricultural biomass. *Coord Chem Rev* 254:2181-2192
- Park Y, Shin WS, Choi SJ (2012) Removal of Co, Sr and Cs from aqueous solution using self-assembled monolayers on mesoporous supports. *Korean J Chem Eng* 29:1556-1566
- Richard D, Delgado Núñez MDL, Schweich D (2010) Adsorption of complex phenolic compounds on active charcoal: Breakthrough curves. *Chem Eng J* 158:213-219
- Simate GS, Ndlovu S (2015) The removal of heavy metals in a packed bed column using immobilized cassava peel waste biomass. *J Ind Eng Chem* 21:635-643
- Swati A, Hait S (2017) Fate and bioavailability of heavy metals during vermicomposting of various organic wastes-A review. *Process Saf Environ* 109:30-45
- Traylor SJ, Xu X, Li Y, Jin M, Li ZJ (2014) Adaptation of the pore diffusion model to describe multi-addition batch uptake high-throughput screening experiments. *J Chromatogr A* 1368:100-106
- Valderrama C, Barios JI, Caetano M, Farran A, Cortina JL (2010) Kinetic evaluation of phenol/aniline mixtures adsorption from aqueous solutions onto activated carbon and hypercrosslinked polymeric resin (MN200). *React Funct Polym* 70:142-150
- Velazquez-Jimenez LH, Pavlick A, Rangel-Mendez JR (2013) Chemical characterization of raw and treated agave bagasse and its potential as adsorbent of metal cations from water. *Ind Crop Prod* 43:200-206
- Vijayaraghavan K, Balasubramanian R (2015) Is biosorption suitable for decontamination of metal-bearing wastewaters? A critical review on the state-of-the-art of biosorption processes and future directions. *J Environ Manage* 160:283-296
- Vilar VJ, Botelho CM, Loureiro JM, Boaventura RA (2008) Biosorption of copper by marine algae *Gelidium* and algal composite material in a packed bed column. *Bioresour Technol* 99:5830-5838
- Xia L, Hu YX, Zhang BH (2014) Kinetics and equilibrium adsorption of copper(II) and nickel(II) ions from aqueous solution using sawdust xanthate modified with ethanediamine. *T Nonferrous Met Soc* 24:868-875

Table 1. Experimental parameters used in the model for prediction of metal ions breakthrough curves.

Interstitial velocity (m·s ⁻¹)	1. 061x10 ⁻⁴
Grape stalks density (Kg·m ³)	92.33
Bed height (m)	6.7x10 ⁻²
Particle radius (m)	3.75x10 ⁻⁴
Metal solution density (Kg·m ³)	998.2
Metal solution viscosity (Kg·m ⁻¹ ·s ⁻¹)	1.002x10 ⁻³

Table 2. Results of model prediction for metal sorption onto grape stalks from ternary mixtures: (a) model parameters, (b) sum of squares residuals (*SSR*) and mean sum of squares residual (*MSSR*). Data obtained in single solutions has been also included for comparison sake, (c).

(a)

Parameter						
Metal	Co-ion	$k_{f,i}$ (cm·s ⁻¹)	$D_{s,ii}$ (cm ² ·s ⁻¹)	$K_{max,i}$ (mmol·g ⁻¹)	b_i (L·mmol ⁻¹)	η_i
Cu	Ni-Cd	2.78 x10 ⁻⁴	0.29 x10 ⁻⁸	0.17	15.00	0.29
	Pb-Cd	2.36 x10 ⁻⁴	0.77 x10 ⁻⁸	0.15	14.98	0.52
	Pb-Ni	1.70 x10 ⁻⁴	8.39 x10 ⁻⁸	0.11	15.52	0.44
Ni	Cu-Cd	2.33 x10 ⁻⁴	1.82 x10 ⁻⁸	0.28	8.04	2.86
	Cu-Pb	8.09 x10 ⁻⁴	72.3 x10 ⁻⁸	1.36	8.30	33.42
	Pb-Cd	5.05 x10 ⁻⁴	1.25 x10 ⁻⁸	0.39	8.05	4.85
Cd	Cu-Ni	2.12 x10 ⁻⁴	1.35 x10 ⁻⁸	0.18	9.53	1.37
	Cu-Pb	3.60 x10 ⁻⁴	1.98 x10 ⁻⁸	0.18	9.29	1.78
	Pb-Ni	2.85 x10 ⁻⁴	3.67 x10 ⁻⁸	0.19	9.54	2.02
Pb	Cu-Cd	6.18x10 ⁻⁴	1.37 x10 ⁻⁸	0.27	54.49	1.97
	Cu-Ni	15.2 x10 ⁻⁴	0.36 x10 ⁻⁸	0.35	54.76	2.85
	Ni-Cd	4.12 x10 ⁻⁴	2.98 x10 ⁻⁸	0.21	54.40	1.21

(b)

Ternary system	<i>SSR</i>	<i>MSSR</i>
Cu - Ni - Cd	6.69 x10 ⁻³	6.03 x10 ⁻⁵
Cu - Pb - Ni	4.58 x10 ⁻³	4.59 x10 ⁻⁵
Cu - Pb - Cd	8.24 x10 ⁻³	7.85 x10 ⁻⁵
Pb - Ni - Cd	5.33 x10 ⁻³	4.68 x10 ⁻⁵

(c)

Metal	K_f (cm·s ⁻¹)	D_s (cm ² ·s ⁻¹)	Q_{max} (mmol·g ⁻¹)	b (L·mmol ⁻¹)
Cu	5.08 x10 ⁻⁴	2.49 x10 ⁻⁸	0.24	15.1
Ni	3.71 x10 ⁻⁴	3.43 x10 ⁻⁸	0.26	8.02
Cd	4.91 x10 ⁻⁴	2.71 x10 ⁻⁸	0.23	9.54
Pb	5.34 x10 ⁻⁴	2.01 x10 ⁻⁸	0.18	54.4

Table 3. Results of sensitivity analysis. SSR_i and VR values of model parameters

		Cu-Ni-Cd		Cu-Pb-Ni		Cu-Pb-Cd		Pb-Ni-Cd	
		<i>SSR_j</i>	<i>VR_j</i>	<i>SSR_j</i>	<i>VR_j</i>	<i>SSR_j</i>	<i>VR_j</i>	<i>SSR_j</i>	<i>VR_j</i>
Cu	$k_{f,i}$	6.70x10 ⁻³	0.16	4.43x10 ⁻³	3.24	8.37x10 ⁻³	1.54		
	$D_{s,ii}$	6.71x10 ⁻³	0.23	4.58x10 ⁻³	0.01	8.25x10 ⁻³	0.06		
	$K_{max,i}$	9.92x10 ⁻³	48.20	7.42x10 ⁻³	61.95	1.19x10 ⁻²	43.93		
	b_i	6.97x10 ⁻³	4.23	5.13x10 ⁻³	11.98	8.93x10 ⁻³	8.30		
	η_i	6.92x10 ⁻³	3.44	5.20x10 ⁻³	13.56	8.83x10 ⁻³	7.11		
Ni	$k_{f,i}$	6.71x10 ⁻³	0.25	4.55x10 ⁻³	0.67			5.37x10 ⁻³	0.69
	$D_{s,ii}$	6.68x10 ⁻³	0.21	4.58x10 ⁻³	0.09			5.34x10 ⁻³	0.09
	$K_{max,i}$	7.27x10 ⁻³	8.72	6.77x10 ⁻³	47.86			6.23x10 ⁻³	16.96
	b_i	7.02x10 ⁻³	4.99	6.42x10 ⁻³	40.10			5.95x10 ⁻³	11.60
	η_i	7.03x10 ⁻³	5.08	6.61x10 ⁻³	44.39			6.00x10 ⁻³	12.61
Cd	$k_{f,i}$	6.71x10 ⁻³	0.34			8.25x10 ⁻³	0.01	5.30x10 ⁻³	0.55
	$D_{s,ii}$	6.68x10 ⁻³	0.17			8.34x10 ⁻³	1.06	5.34x10 ⁻³	0.23
	$K_{max,i}$	8.20x10 ⁻³	22.57			9.90x10 ⁻³	20.06	7.87x10 ⁻³	47.64
	b_i	7.13x10 ⁻³	6.52			8.68x10 ⁻³	5.22	6.15x10 ⁻³	15.34
	η_i	7.10x10 ⁻³	6.13			8.61x10 ⁻³	4.41	6.07x10 ⁻³	13.87
Pb	$k_{f,i}$			4.57x10 ⁻³	0.31	8.21x10 ⁻³	0.48	5.33x10 ⁻³	0.09
	$D_{s,ii}$			4.57x10 ⁻³	0.11	8.25x10 ⁻³	0.07	5.33x10 ⁻³	0.04
	$K_{max,i}$			6.48x10 ⁻³	41.44	1.12x10 ⁻²	35.86	1.21x10 ⁻²	126.75
	b_i			5.61x10 ⁻³	22.40	9.25x10 ⁻³	12.11	5.88x10 ⁻³	10.39
	η_i			5.58x10 ⁻³	21.95	9.16x10 ⁻³	11.02	5.83x10 ⁻³	9.45

Table 4. Results of model sensitivity towards experimental errors.

		Cu-Ni-Cd $\bar{x} \pm s$	Cu-Pb-Ni $\bar{x} \pm s$	Cu-Pb-Cd $\bar{x} \pm s$	Pb-Ni-Cd $\bar{x} \pm s$
Cu	$k_{f,i}$	$(2.764 \pm 0.017) \times 10^{-4}$	$(1.577 \pm 0.188) \times 10^{-4}$	$(2.306 \pm 0.729) \times 10^{-4}$	
	$D_{s,ii}$	$(0.272 \pm 0.017) \times 10^{-8}$	$(7.166 \pm 4.217) \times 10^{-8}$	$(0.785 \pm 0.227) \times 10^{-8}$	
	$K_{max,i}$	0.171 ± 0.003	0.111 ± 0.008	0.143 ± 0.009	
	b_i	15.008 ± 0.008	15.478 ± 0.193	15.044 ± 0.055	
	η_i	0.280 ± 0.014	0.344 ± 0.016	0.405 ± 0.019	
Ni	$k_{f,i}$	$(2.376 \pm 0.071) \times 10^{-4}$	$(9.240 \pm 1.430) \times 10^{-4}$		$(5.270 \pm 0.025) \times 10^{-4}$
	$D_{s,ii}$	$(1.768 \pm 0.082) \times 10^{-8}$	$(56.260 \pm 34.673) \times 10^{-8}$		$(1.178 \pm 0.006) \times 10^{-8}$
	$K_{max,i}$	0.284 ± 0.007	1.301 ± 0.044		0.443 ± 0.002
	b_i	8.041 ± 0.010	8.499 ± 0.202		8.053 ± 0.007
	η_i	2.851 ± 0.028	32.369 ± 0.814		5.706 ± 0.004
Cd	$k_{f,i}$	$(2.101 \pm 0.053) \times 10^{-4}$		$(2.719 \pm 0.548) \times 10^{-4}$	$(2.991 \pm 0.052) \times 10^{-4}$
	$D_{s,ii}$	$(1.338 \pm 0.174) \times 10^{-8}$		$(2.174 \pm 0.344) \times 10^{-8}$	$(3.856 \pm 0.078) \times 10^{-8}$
	$K_{max,i}$	0.180 ± 0.005		0.182 ± 0.013	0.184 ± 0.001
	b_i	9.528 ± 0.013		9.377 ± 0.128	9.537 ± 0.004
	η_i	1.353 ± 0.050		1.707 ± 0.035	2.011 ± 0.015
Pb	$k_{f,i}$		$(15.148 \pm 0.162) \times 10^{-4}$	$(4.881 \pm 2.046) \times 10^{-4}$	$(4.368 \pm 0.087) \times 10^{-4}$
	$D_{s,ii}$		$(0.551 \pm 0.255) \times 10^{-8}$	$(1.243 \pm 0.600) \times 10^{-8}$	$(2.769 \pm 0.082) \times 10^{-8}$
	$K_{max,i}$		0.390 ± 0.019	0.288 ± 0.015	0.216 ± 0.000
	b_i		54.809 ± 0.138	54.429 ± 0.029	54.412 ± 0.027
	η_i		2.711 ± 0.016	1.735 ± 0.014	1.293 ± 0.009

Figure 1. Experimental data and predictive breakthrough curves for metal sorption onto GS from ternary systems: a) Cu-Ni-Cd, b) Cu-Pb-Cd, c) Cu-Pb-Ni, d) Pb-Ni-Cd. Flow rate: 30 mL·h⁻¹; feeding metal concentration: 0.2 mM; pH: 5.2; sorbent mass: 0.5 g; particle size: 0.25-0.50 mm.

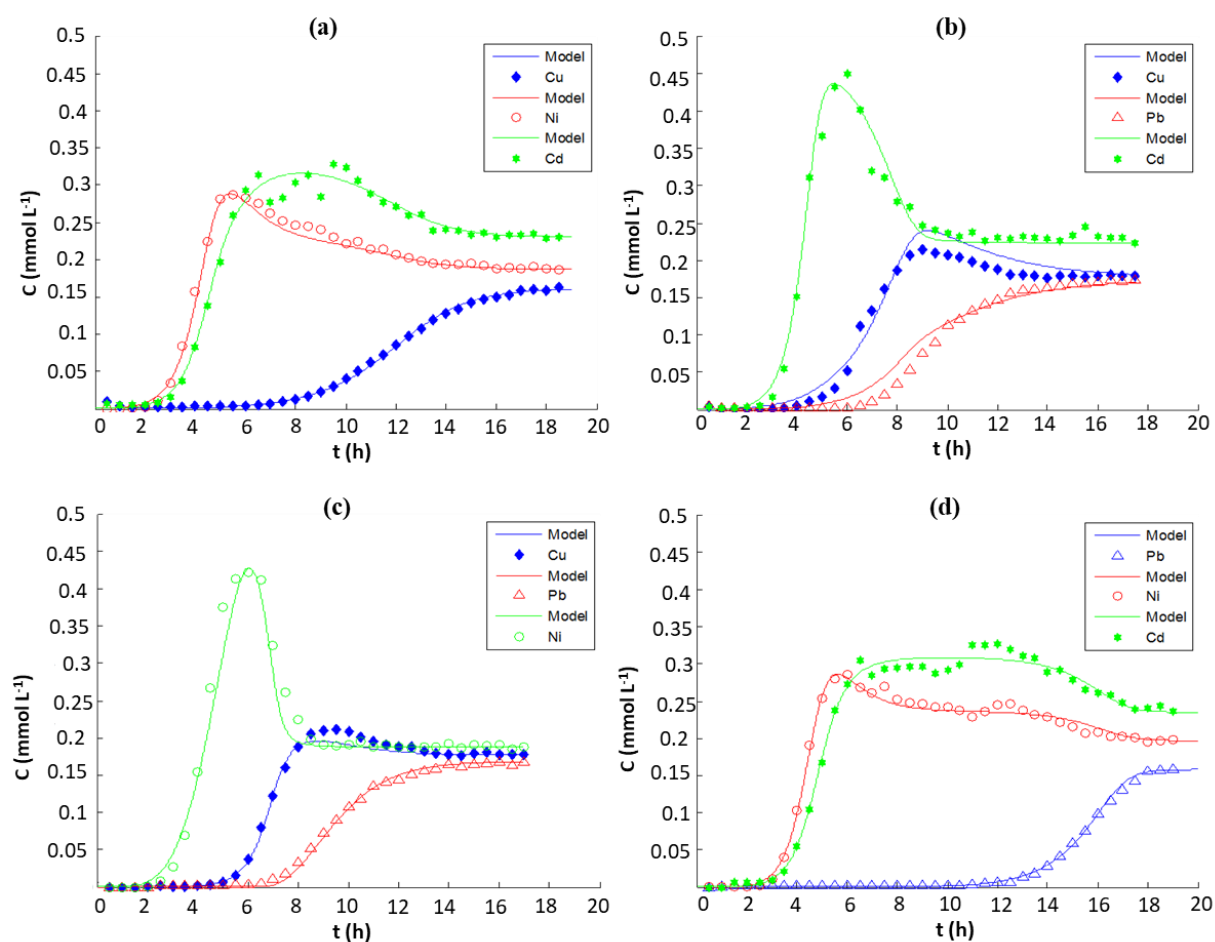


Figure 2. Metal sorption onto grape stalks from ternary systems as a function of time: a) Cu-Ni-Cd, b) Cu-Pb-Cd, c) Cu-Pb-Ni, d) Pb-Ni-Cd. Flow rate: 30 mL·h⁻¹; feeding metal concentration: 0.2 mM; pH: 5.2; sorbent mass: 0.5 g; particle size: 0.25–0.50 mm.

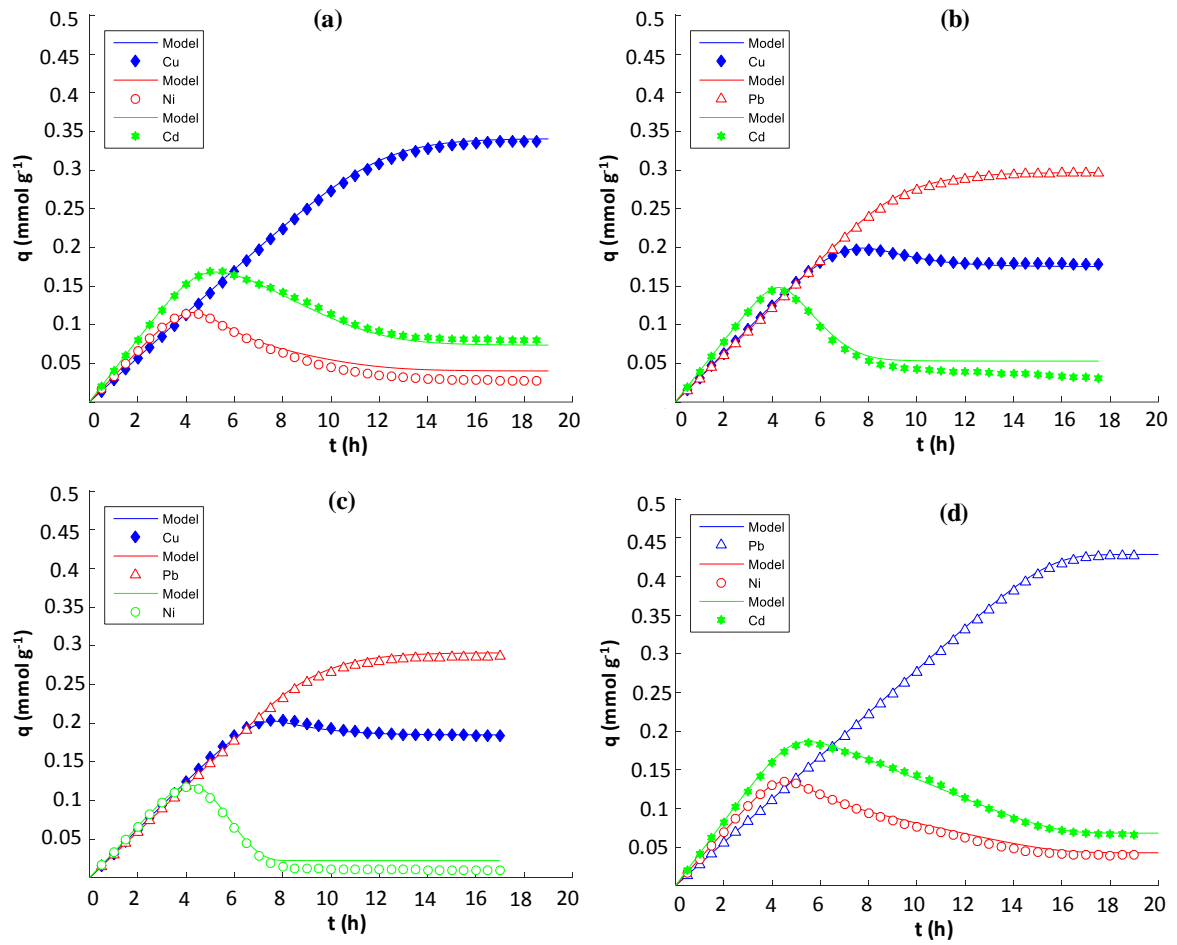


Figure 3. Experimental and calculated values of the sorbed amount of each metal ion at equilibrium

